GAS SOLID CONTACTING MEASUREMENTS IN A TURBULENT FLUIDIZED BED BY OXIDATION OF CARBON MONOXIDE

by

Robbie H. VENDERBOSCH[a*], Wolter PRINS[a,b], and Wim P. M. Van SWAAIJ[c]

[a] BTG Biomass Technology Group B.V., Enschede, The Netherlands
[b] Ghent University, Ghent, Belgium
[c] University of Twente, Enschede, The Netherlands

Original scientific paper
https://doi.org/10.2298/TSCI180727291V

The conversion rate of the mass transfer controlled oxidation of CO over a Pt/γ-alumina catalyst (d_p = 65 μm) has been studied in a fluidized bed (internal diameter = 0.05 m) operated close to and in the turbulent fluid bed regime. The objectives were to investigate the gas-solids contacting efficiency to evaluate the conversion data in terms of overall mass transfer coefficients and define the apparent contact efficiency. At high superficial gas velocities, the concept of formation of particle agglomerates and voids is more realistic than the two-phase model considering discrete bubbles and a dense phase. The two-phase model is not useless but has hardly any relation with the real flow pattern in the turbulent regime.

Key words: *turbulent fluidized bed, mass transfer, CO oxidation, contacting efficiency*

Introduction

Fluid bed reactors are among others applied in the chemical industry when dealing with fast exothermic or regenerative heterogeneous reactions. When high through-put capacities and small reactor diameters are required (for example for high pressure processes), high-velocity fluidization is often considered to be a very good alternative for the more conventional (bubbling) fluidized bed. In this paper, the term high velocity fluid bed is used to describe the fluidization regime going from gas velocities well above the minimum bubbling velocity up to the transport velocity of the particles. For the particles applied in this work, with d_p = 65 [μm] and ρ_p = 1375 [kgm^{-3}], this is in between 0.2< u_g <1 [ms^{-1}]. Most of the fluid bed cat cracking regenerators, for example, operate in this regime.

The high velocity fluid bed (*a.o*. the turbulent fluid bed) is supposed to offer unique properties for gas-solids reactions. The advantages claimed for the high-velocity fluidized beds over the conventional bubbling fluidized beds are the better gas-solids contacting due to the absence of well-defined bubbles, the decrease in gas back-mixing and the higher gas through-put. Most of these advantages are directly related to the use of small particles, but also to the increased solids hold-up in the freeboard of the reactor. An important claim concerns a better gas-solids contacting. However, where most research in fluidized bed concentrates on hydrodynamics, limited information is available on the actual gas-solids contacting in high velocity fluid beds. The contact efficiency of gas-solids in a circulating fluidized bed (CFB) is not well understood, because of measurement difficulties but als because of the lack of a rigorous definition for the

* Corresponding author, e-mail: venderbosch@btgworld.com

contact efficiency. A better understanding thus will help in the design of such reactors. This paper attempts to present some of the efforts made in developing a better understanding of the gas-solids contact efficiency, especially in turbulent fluid bed reactors. For this, experimentally determined mass transfer data are collected from a series of experiments using the oxidation of CO.

Gas-solid contact efficiency

The gas-solids contacting determines to what degree the observed conversion rate deviates from the maximal possible conversion rate, which is derived by assuming all the particles to be ideally contacted by the reactant gas. For first order reactions, the contact efficiency, η, can be defined as the apparent reaction rate constant (here k_{ov}) over the theoretical maximum or intrinsic reaction rate constant (here taken as k_p), $\eta = k_{ov}/k_p$. The value η here includes effects of conversion-rate controlling resistances except those inside the single particle. Values considerably lower than one are observed for various gas-solids reactors. For a bubbling fluid bed, the conversion rate is affected by another clear mass transfer resistance, which is due to the bubbles, and in riser systems the conversion rates are affected by the transfer of reactant from the gas bulk to particle agglomerates and inside the agglomerates. The turbulent fluid bed presents aspects of both these fluid beds and in case of a very fast reaction, a reduction in contacting efficiency should be recognizable from unexpected low values for the derived overall mass transfer numbers. Compared to the large body of empirical information/correlations available for the case of bubbling beds, empirical information available for fast-fluidized bed reactors and turbulent fluidized bed reactors is much less and more scattered [1]. The CFD calculations on turbulent beds are scarce [2-5]. Notwithstanding the commercial interest in and the use of turbulent fluidized beds, to our knowledge no studies regarding the relation between the conversion and mass transfer limitation for turbulent beds are published in the open literature. Benefits expected in such fluidized bed reactors include significantly reduced gas and solids backmixing, improved contact efficiency, and continuous process coupled with higher product capacity. However, result of the contact efficiency shows that the CFB riser is far away from an ideal plug flow reactor [3]. The presence of interparticle forces in the gas-solid fluidized bed leads to a significant modification of the bed hydrodynamics, affecting the the distribution of the fluidizing gas between the bubble and emulsion phases [4, 5].

In the present paper, experimentally determined mass transfer data are collected from a series of experiments using the oxidation of CO. This oxidation, over a platinum based catalyst, offers advantages over other model reactions. When going from a kinetically controlled reaction at low temperatures to mass transfer controlled reaction at the higher temperatures, a shift in the apparent order in CO will be observed, viz. from a negative value to plus one. In addition, upon arriving in the mass transfer controlled regime, the apparent activation energy decreases to a value in line with the temperature dependency of diffusional transport. Preceding the discussion of the experimental work and interpretation of the measurements, a review of ideas and observations regarding turbulent fluid bed performance is presented in the subsequent section.

High velocity fluidized bed reactor performance

A fluid bed of fine particles has well defined bubbles (the bubbling bed) at low gas velocities, but this bubble structure is destroyed if the velocity is substantially increased (the turbulent bed). In the latter shapeless voids, distributed over the bed volume appear and disappear with high frequency, and a main feature is its overall pseudo-homogeneous appearance. The fluid bed then shows periods during which there are massive solid structures in the bed, containing rising gas packets, and periods in which the gas is present as the continuous phase with dispersed

particles clusters [6]. Good gas-solids contacting is suggested for turbulent fluidized beds and this is primarily based on the absence of well-defined bubbles which fact facilitates the transfer of reactant from the bulk gas to the reactive particles. Nevertheless, pertinent data for mass transfer coefficients in turbulent beds are not available. Besides, the number of papers in the literature dealing with a chemical reaction in a turbulent bed, is limited. Due to the lack of understanding of the physical nature of this fluid bed regime, any interpretation of conversion data is troublesome. Usually conversion results are interpreted by using the two-phase model or by a simpler axial dispersion model. The latter model, for the turbulent bed regime used by Edwards and Avidan [7] and Foka *et al*. [8], is problematic because it does not predict conversions lower than those obtained for an ideally mixed reactor, while at the same time reactant by-passing (*e.g*. via the bubbles in the bubbling bed) is known to be the cause of such low conversions. A better approach would then be to describe the conversion data in terms of a two-phase model.

In the two-phase model concept the limited gas-solids contacting is explained by the by-passing of reactant gas through bubbles (clearly visible in a bubbling bed). The main assumptions of the simplified two-phase model are that there are no solid particles in the bubble phase, and the bubble phase passes in plug flow through the reactor. Interpretation of conversion data in the two-phase model showed that for high reaction rate constants the mass transfer apparently becomes better. Possible explanations are the chemical enhancement of the bubble-to-dense phase mass transfer, and additional reaction taking place within the bubbles or in the disengagement zone. The simple approach of a two-phase model plus chemical reaction in series is only valid up at low reaction rates, while chemical enhancement of mass transfer should be taken into account for the higher reaction rates [9].

The performance of turbulent fluidized bed reactors, however, is still unclear, interpretation of conversion data reported in the literature can be carried out on basis of the two-phase model (although there is no well-defined bubble and dense phase structure), or on basis of the axial dispersion model (which is unable to predict conversions lower than those of an ideally mixed tank reactor). Models are developed to take into account the effects of meso-scale structures (*i.e*. bubbles) to improve *coarse-grid* simulation of bubbling and turbulent fluidized beds. These models are extended to account for the hydrodynamic disparity between homogeneous and heterogeneous fluidization by correlating it with both local voidage and slip velocity [10]. In other approaches different drag models are proposed to taken into account additional energy dissipation from forming heterogeneous structures [11, 12].

An simpler approach useful in riser set-ups is interpreting the conversion data on basis of a concept, which assumes the presence of clusters of particles (agglomerates) in the bed, instead of the presence of distinct bubbles. The experimental work in the present paper is based on the oxidation of CO over a platinum on γ-alumina catalyst [13, 14]. A specific feature of this reaction system is that the local conversion rate can be varied by diluting the active catalyst with inert bed material, and that the overall reaction rate in CO is –1 for kinetic controlled conditions and +1 for mass transfer limited conditions, see the general reaction rate expression [13]:

$$R(c) = \frac{k_p^{\,0} \exp\left(-\frac{E_a}{\mathrm{R}T}\right) c c_{O2}}{\left[1 + K_a^{\,0} \exp\left(-\frac{\Delta H_a}{\mathrm{R}T}\right) c\right]^2} \tag{1}$$

where c and c_{O2} representing the CO and O_2 concentration, respectively, $k_p^{\,0}$ and $K_a^{\,0}$ the reaction constants, and E_a and ΔH_a the activation and adsorption energies, respectivity. In our previous

work on dense fluid beds and risers the conversion results were analysed according to various methods, amongst which the two-phase model and the cluster model. The dominating rate controlling mechanism in these concepts is supposed to be the mass transfer rate.

Experimental conditions

In the mass transfer controlled conversion experiment a platinum-based catalyst has been used, and pure Geldart's A γ-alumina was used as the inert bed material (particle diameter d_p = 65 μm, particle density ρ_p = 1375 kg/m^3 and particle terminal falling velocity at ambient conditions u_t = 0.16 m/s). The amount of solids in the reactor ranged from approximately 150 to 200 g depending on the applied gas velocity.

The oxidation of CO is performed in the lab-scale turbulent fluidized bed facility, fig. 1. More details on the unit can be found elsewhere [15]. The set-up consists of: a gas mixing section to provide the required gas mixture for the oxidation reaction, a heated turbulent fluidized bed section, and an analysis section for continuous CO and CO_2 monitoring by two Maihak analyzers. The turbulent fluidized bed (0.05 m internal diameter, 0.75 m in height) is equipped with an expanded top bed (0.10 m internal diameter, 0.30 m height), both made of quartz. The fourfold area increase in the expanded top section reduces the superficial gas velocity, which allows most of the entrained particle to fall back in the bed. Two cyclones, with internal diameters of 63 mm and 50 mm are applied to separate the entrained solids from the gas. The solids are returned to the fluidized bed by means of an external dip-leg. To ensure smooth operation of the dip-leg, a very small amount of nitrogen (approximately 2 ml/s) was introduced at its bottom. In all experiments, the conversion of CO was measured at the exit of the reactor (including the bed and the disengagement zone). Mass-flow controllers have been applied to adjust the superficial gas velocity in the reactor, and the gas stream compositions. Gas velocities were in the range of 0.1 to 1 m/s, and the oxygen concentrations in the gas inlet could be varied from 8 to 12 vol.%, whereas CO concentrations were in the range of 0.2 to 1 vol.% (balance N_2). The fluidized bed set-up was operated at ambient pressures, and placed in an electrical column oven to enable operating temperatures up to 1200 K. A series of thermocouples was positioned along the riser wall to measure and control the reactor temperature. The oven was further equipped with a spy-glass for visual observation of the fluidization behaviour in the reactor. The axial pressure profile could be recorded at any time by a series of pressure taps along the fluid bed column.

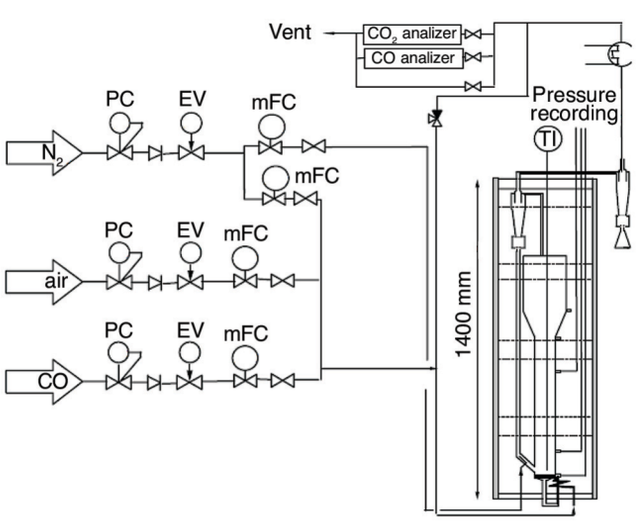

Figure 1. Schematic representation (non-scale) of the lab-scale turbulent fluidized bed

The temperature in the present oxidation experiments was varied from 575 to 775 K, while the active material could be diluted in ratios varying from n_d = 5058 to 30560. Lower dilution ratios could not be applied because that would result in too high conversions (close to 1) and possible errors in the analysis of

the reaction gas. The experiments were carried out from high to lower dilution ratios, ensuring that very small amounts of active material, inevitably remaining in the reactor, do not affect the subsequent conversion experiments. The results of all measurements were reproducible, and prior to further experimental work, it was observed that the inert material, pure γ-alumina, was indeed inactive in the oxidation of CO within the range of operating temperatures, deactivation of catalyst does not occur.

Results

First the axial solids concentration profile has been determined in the small turbulent fluidized bed set-up at various operating conditions. As the contribution of the acceleration term to the total pressure drop can be neglected if compared with the solids hold-up contribution, the solids hold-up β can be calculated directly from the observed pressure drop over the bed height, z.

At higher temperatures the hold-up in the dense region (at the bottom of the bed) is decreased in favour of the hold-up in the dilute region (the freeboard), fig. 2. The terminal falling velocity of the individual particles decreases at the higher temperature, due to the effect of temperature on the viscosity. If the size and density of particle agglomerates is assumed to be independent on the temperature, the terminal falling velocity of the agglomerate is also expected to decrease at higher temperatures. Consequently, more agglomerates will be entrained by the fluidization gas, leading to an increased solids concentration in the freeboard.

For the oxidation reaction of CO with oxygen over a Pt / γ-alumina catalyst parameters influencing the conversion in a reactor are the gas velocity, the CO (y_{in}) and O_2 (y_{O2}) inlet fractions, the reaction temperature and the dilution ratio n_d. The solids concentration cannot be varied in a bubbling or turbulent fluid bed, at a given temperature, particle and bed properties it is determined almost exclusively by the gas velocity.

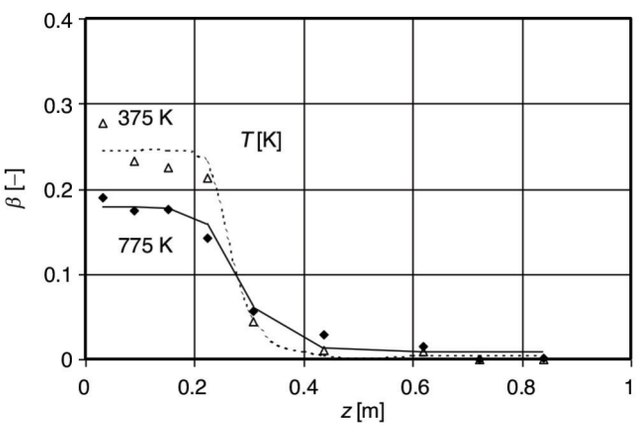

Figure 2. The axial solids hold-up profile for two temperatures and a gas velocity of 0.6 m/s. Legends: Δ375 K; ♦ 775 K. The lines are trendlines

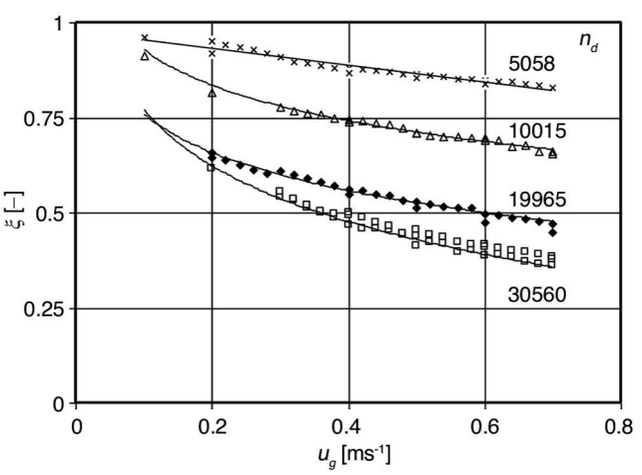

Figure 3. The CO conversion *x vs.* the superficial gas velocity u_g for various dilution ratios n_d at a reactant inlet fraction of 0.5 vol.% CO and a oxygen inlet fraction of 10 vol.%, T = 775 K. Legends: x n_d = 5058, Δn_d = 10015, ♦n_d = 19965, and □n_d = 30560

Figure 3 shows the CO conversion $\xi = 1 - y_{out}/y_{in}$ plotted *vs*. the gas velocity for various dilution ratios, n_d = 5088 up to n_d = 30560. Assuming plug flow behaviour of the gas, the conversion decreases exponentially with increasing gas velocity, due to the shorter contact time. At lower dilution ratios (viz. more active material) the conversion increased. Whether the conversion is controlled by mass transfer or the reaction kinetics can easily be verified by the observed order in CO and O_2, and by the apparent activation energy.

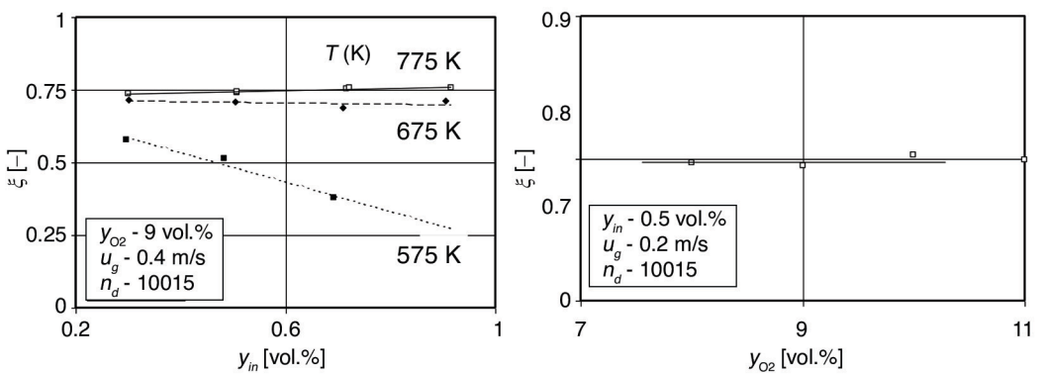

Figure 4. (a) The CO conversion ξ *vs*. the CO inlet fraction y_{in} for a dilution ratio n_d = 10015, u_g = 0.4 m/s and (b) the CO conversion *vs*. the oxygen inlet fraction y_{O2}, n_d = 10015, u_g = 0.2 m/s, T = 675 K (b). Legends: □ 775 K, ♦ 675 K, ■ 575 K

Figure 4 presents the conversion ξ as a function of the CO inlet concentration, y_{in}, for 3 operating temperatures and for the relatively low superficial gas velocities u_g < 0.4 m/s. At a temperatures of 575, the conversion decreases clearly with increasing inlet fractions of CO, pointing at an apparent reaction order in carbon monoxide below 1. The apparent order increases at the higher temperatures. From 675 K, the conversion becomes independent of y_{in}, suggesting that the reaction rate is mass transfer controlled at this temperature level. In fig. 4(b) the conversion of CO is plotted as a function of y_{O2}, the volume fraction O_2. Again, at the high temperature level, the oxygen inlet concentration does not affect the conversion anymore, and a zero order in oxygen is therefore plausible from 675 K. The apparent order in CO and in O_2, are then in accordance with the values that are expected if mass transfer is the rate controlling step [13].

Starting from these first and zero-order kinetics in the reactant concentration, *c*, (CO or O_2 resp.), the apparent reaction rate constant per unit volume of catalyst k_{ov} can be derived easily from a pseudo-homogeneous approach, while assuming plug flow behaviour of the gas, and neglecting the axial dispersion of the gas:

$$\frac{\partial u_g A c}{\partial x} = -k_{ov} c \frac{\beta A \Delta L}{(1+n_d)} \Rightarrow k_{ov} = -\frac{u_g(1+n_d)}{\beta \Delta L} \ln\left(\frac{c_{out}}{c_{in}}\right) \tag{2}$$

In fig. 5 the apparent reaction rate constant, k_{ov}, is plotted *vs*. the inverse operating temperature for various gas velocities. The data points in this plot have been obtained at a dilution ratio n_d = 30560. At the higher temperatures and gas velocities a significant increase in k_{ov} is observed. From the slopes of the curves over the temperature range of 675 to 775 K, an apparent activation energy of E_a = 12 to 16 kJ/mole can be derived for all nd-values. They appear to be almost independent on the gas velocity. In fig. 5(b) a similar plot is presented, but now for a lower dilution ratio n_d = 10015. The apparent activation energy appears to depend only slightly on the gas velocity: its value ranges from 8 kJ/mole at u_g = 0.6 m/s to 4 kJ/mole for u_g = 0.1 m/s. Two major observations result from the comparison of figs. 5(a) and 5(b). At the lowest dilution ratio

fig. 5(b), a stronger influence of the gas velocity on the apparent reaction rate constant is observed, and a decreased activation energy, both indicating a somewhat more pronounced effect of mass transfer limitation. Nevertheless, the low values for the activation energy suggest that for both dilution ratios, the mass transfer mainly controls the conversion rate. This is confirmed by the first order in the CO concentration at the higher temperatures for all n_d - values applied in the present work.

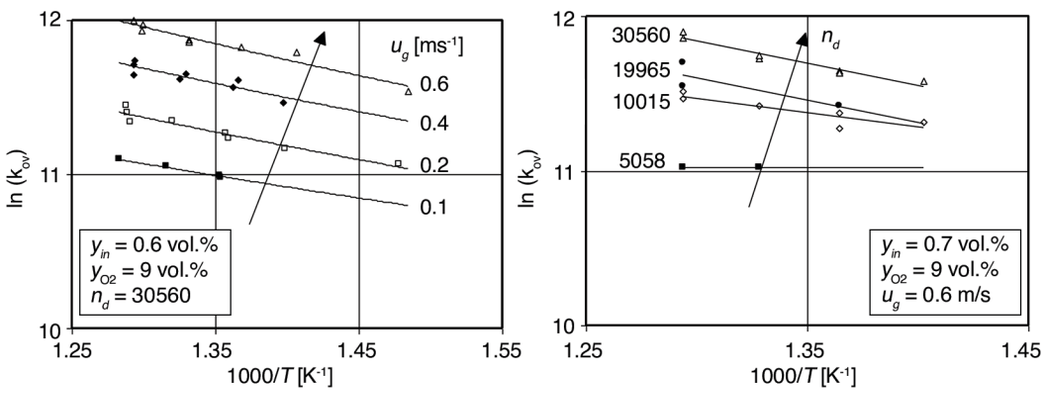

Figure 5. Dependency of the observed apparent rate constant on the operating temperature and the gas velocity for a dilution ratio of (a) n_d = 30560 and (b) n_d = 10015 and a reactant inlet fraction y_{in} = 0.6 vol.%

In fig. 6, the effect of the dilution on the apparent rate constant is further illustrated. It shows that kov increases with increasing temperature and dilution ratio, the latter effect being more pronounced at the higher temperatures.

At higher temperatures the reaction becomes first order in the CO concentration, and the order in the oxygen concentration approaches zero. The apparent activation energy for n_d = 30560 approaches a value of E_a = 12 kJ/mole, which is close to the one that can be derived for gas-phase diffusion ($\cong$11 kJ/mole). As an additional observation, these three effects appear to be more pronounced at lower dilution ratios, viz. when the (local) reaction rate increases. These observations together indicate that mass transfer is the reaction rate controlling step at temperatures above 675 K.

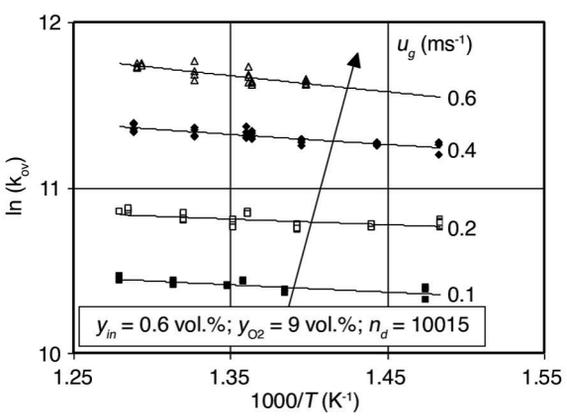

Figure 6. Dependence of the logarithmic apparent rate constant k_{ov} on the reciprocal operating temperature T and the dilution ratios n_d for a reactant inlet concentration y_{in} = 0.7 vol.%, and u_g = 0.6 m/s

Effects of the gas velocity and the dilution ratio on apparent Sherwood numbers

For the reaction rates completely controlled by mass transfer, the Sherwood number can be derived from the apparent kinetic rate constant, k_{ov}. Assuming spherical particles, the apparent Sherwood number, Sh = $k_{ov}\, d_p^2/(6D)$, with D the molecular diffusion coefficient. Figure 7 shows

the Sherwood number as a function of the gas velocity for all four dilution ratios applied. The apparent Sherwood number becomes higher for higher gas velocities and higher n_d.

Interestingly, despite the high dilution ratios applied, the apparent Sherwood numbers are lower than expected on basis of ideal contacting of a spherical particle (Sh = 2). The decrease with a factor 2 to 10, depending on the applied gas velocity and dilution ratio, is comparable with the results obtained in a small riser [14].

Discussion and comparison with previous work

Mass transfer data in various reactors can be compared in a plot of the Sherwood number *vs*. the particle Reynolds number, the latter being defined on basis of the slip velocity between the solids and gas. In fig. 8 the data published for packed and bubbling fluidized beds are represented by the shaded area. The mass transfer numbers calculated in the present work are presented in two curves (denoted by 4 in fig. 8), one for a dilution ratio of n_d = 5058, and the other for n_d = 30560. These data are much higher than those for packed and bubbling fluidized beds, but somewhat lower than the Sherwood numbers for individual particle contacting (curve 1), represented by the Ranz-Marshall equation [16, 17]. At higher Reynolds numbers (corresponding with higher gas velocities), and high dilution ratios the observed mass transfer number approaches this ideal case, but still remains somewhat lower (perhaps due to shielding of the active surface area by surrounding inert particles).

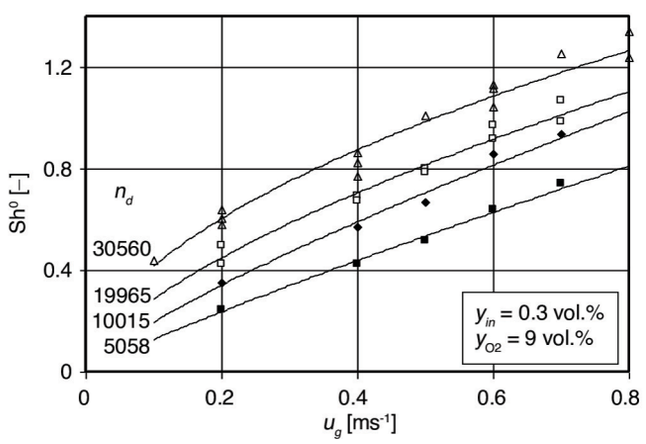

Figure 7. The dependence of the apparent Sherwood number on the gas velocity for various dilution ratios n_d and an operating temperature of 775 K.

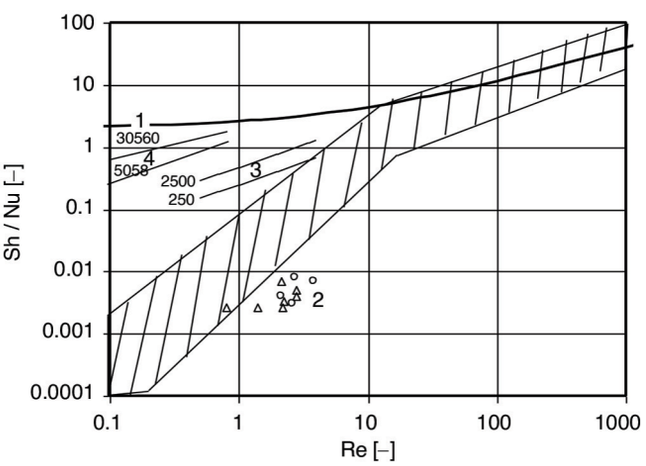

Figure 8. Sherwood and Nusselt numbers as a function of Reynolds number in fluidized beds. Literature data for fluidized beds and packed beds are indicated [13]. Legend: Ranz-Marshall [10,11]; Δ Van der Ham [12], ○ Van der Ham [12]; CO oxidation experiments in a riser [8]; The present work: for n_d = 5058 and n_d = 30560

Gas-to-particle mass (or heat) transfer data for the turbulent flow regime are not readily available in the literature, and our data are compared with mass transfer data in other reactor types. For comparison the riser data of Van der Ham [18], as well as our own data for a riser of a CFB are presented in fig. 8 (triangles, circles and curve 3 respectively) [14]. Despite the lower gas velocities applied in

this work, and consequently lower Reynolds numbers, the apparent Sherwood numbers in the turbulent regime are significantly higher than those obtained in the riser of a CFB set-up. This is almost certainly due to the higher degree of dilution in the present work. It is important to note that the apparent Sherwood numbers as observed here only reflect overall values, in which (amongst others) the bubble-to-dense phase or gas-to-cluster mass transfer resistance are lumped. Obviously, the mass transfer data should be handled with great care, the more so because in industrial reactors dilution of the active catalyst is seldom applied.

The conversion rate obviously is controlled by mass transfer resistances. In the ideal case, the mass transfer resistance is located entirely in the particle boundary-layer. The theoretical maximum can be calculated from the reaction rate that is observed when only the mass transfer resistances on a particle level are important, or in other words, as if the particles are ideally contacted by the gas. For that extreme case, the value for the theoretical maximum apparent reaction rate corresponds with $k_{ov} = k_g a$, and can be derived from the Ranz-Marshall equation. Here k_g is the mass transfer coefficient and a the specific surface, both taken for the single particle.

The contact-efficiency can now be calculated from the conversion data as the ratio between the observed Sherwood number and the one derived by Ranz and Marshall, and a comparison with literature data can be done by plotting the contact efficiency values *vs*. the reaction number N_r, defined by $N_r = k_p \beta \tau / (1+n_d)$, fig. 9.

Figure 9 shows that the apparent contact efficiency strongly decreases with increasing reaction number. Contact efficiencies in the range of $0.2 < \eta < 0.8$ are now calculated, which is in fair agreement with the trends in contact efficiency data published [3, 19-21]. The dashed line indicates the curve of the contacting efficiency that can be calculated if the gas phase of the fluid bed is supposed to be ideally mixed and the gas-solids contacting to be as expected for an isolated single particle. Our data points are below the CISTR curve for the low gas velocities, and above for the higher gas velocity of 0.7 m/s. At the lowest gas velocities, the contacting is even worse than for the extreme (and unrealistic) case of the ideal mixed tank model. Obviously, the strong decrease cannot be explained by axial dispersion only. Similar behaviour has been observed for bubbling fluidized beds. It is surprising (and not always recognized) that the contact efficiency remains relatively poor over the total range of the gas velocities applied for fluidizing the fine particles.

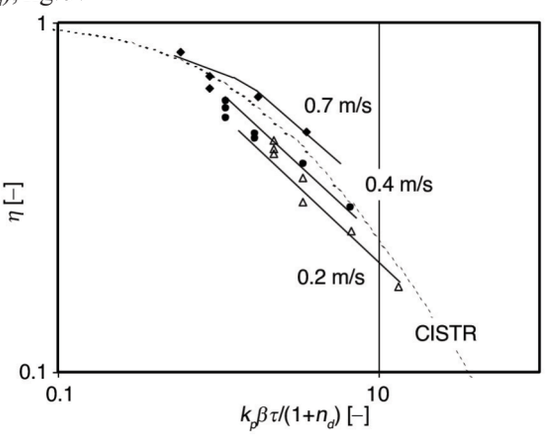

Figure 9. The contact efficiency, η, as a function of the reaction number for various gas velocities at a temperature of 775 K. The dashed line represents the contact-efficiency in the extreme case that an ideal stirred tank model is applied for the gas phase instead of the suggested plug flow behaviour, and only plotted as a reference case. Legends: Δu_g = 0.2 ms^{-1}, $\bullet u_g$ = 0.4 m s^{-1}, and $\blacklozenge$ u_g = 0.7 m s^{-1}. The solid lines are trendlines

Conclusions

In a turbulent fluidized bed mass transfer controlled oxidation experiments of CO over a *Pt* / γ-alumina were conducted to investigate the gas-solids contacting. Similar to observations

reported for packed beds, dense fluidized beds and risers [14], the mass transfer controlled reaction rates could be verified by a low value for the apparent activation energy and a change in the apparent order in the reactant concentrations.

The conversion results are interpreted as overall mass transfer coefficients in the well-known Sherwood versus Reynolds diagram to allow a comparison with published mass transfer data for packed beds, dense fluidized beds and risers. The following conclusions can be summarised:

- Turbulent fluidized beds are well suited to carry out fast reactions, specifically while deploying relatively small particles (Geldart A powders) in reactions that are controlled by mass transfer resistances. Mass transfer rates in these reactors can be high but are much lower than expected on basis of ideal contacting of the individual particles. This mass transfer is difficult to model for turbulent fluidized beds due to the complexity of the phenomena occuring.
- The derived Sherwood numbers are merely overall values, in which the bubble-to-dense phase or mass transfer resistances to and inside the particle agglomerates are lumped. They do not represent the mass transfer rate on the scale of the individual particles, and depend on the dilution ratio.
- The contact-efficiency depends strongly on the local conversion rate. This conclusion could be derived also from the conversion experiments presented by other investigators. Unfortunately, from the diagram of the contact-efficiency versus the reaction number, no additional information is obtained about the rate controlling step.

Just like in the case of a riser regime, for stationary fluid bed operated at the higher gas velocities (that is in the turbulent bed), the particulate phase is structured in agglomerates of various sizes that are frequently formed and disintegrated. Additional mass transfer resistances are then located at both sides of the interface between the bulk gas and the particle agglomerates, that is in the boundary layer around the agglomerate, and inside the agglomerates.

Nomenclature

A – cross-sectional area of the reactor, [m^2]
a – aspecific surface particle, [m^{-1}]
c – CO concentration, [molem^{-3}]
c_{in} – reactant concentration inlet, [molem^{-3}]
c_{O2} – oxygen concentration, [molem^{-3}]
c_{out} – reactant concentration outlet, [molem^{-3}]
D – molecular diffusion coefficient, [m^{2}s^{-1}]
d_p – average particle diameter, [m]
E_a – activation energy defined by eq. (1), [Jmole^{-1}]
H – expanded bed height, [m]
ΔHa – adsorption energy defined by eq. (1), [Jmole^{-1}]
K_a^0 – reaction constant defined by eq. (1), [m^{3}mole^{-1}]
k_g – mass transfer coefficient, [ms^{-1}]
k_{ov} – measured reaction rate based on catalyst volume, [s^{-1}]
k_p – intrinsic reaction rate constant, [s^{-1}]
k_p^0 – reaction rate constant, defined by eq. (1), [m^3 mole^{-1}]
N_r – reaction number, $\{=k_p\,\beta H/[(1+n_d)u_g]\}$, [–]
n_d – dilution ratio, [–]
ΔL – length of the reactor, [m]
R – gas constant, [Jmole^{-1}K^{-1}]
$R(c)$ – reaction rate, [molem^{-3}s^{-1}]
Re – Reynolds number, $(=\rho_g u_g d_p/\eta_g)$ [–]
Sh – experimentally observed Sherwood number, $[=k_{ov}\,d_p^2/(6D)]$ [–]
T – operating temperature, [K]
u_c – transition velocity for the onset of turbulent fluidization, [m s^{-1}]
u_g – superficial gas velocity, [m s^{-1}]
x – non-dimensional axial co-ordinate, $(= z/H)$ [–]
y_{in} – inlet fraction CO, [vol.%]
y_{O2} – inlet fraction oxygen, [vol.%]
z – zaxial position, [m]

Greek symbols

β – solids concentration, [–]
η – contact efficiency $(=k_{ov}/k_p)$ [–]
η_g – gas viscosity, [Pas]
ρ_g – gas density, [kgm^{-3}]
ρ_p – particle density, [kgm^{-3}]
ξ – conversion, [–]
τ – contact time, $(=H/u_g)$ [s]

Acknowledgement

We acknowledge the financial support of the Dutch Ministry of Economic Affairs through the Netherlands Energy Research Foundation ECN. We also thank R. de Wit and E. Middelink for their assistance in the experimental work. We are also obliged to Prof. J.R. Grace and Prof. J. Chaouki for providing us their experimental data.

References

[1] Ranade, V. V., *12 Fluidized Bed Reactors, in Process Systems Engineering*, Academic Press, New York, USA, 2002
[2] Ullah, A., *et al*., Bubble-Based EMMS Mixture Model Applied to Turbulent Fluidization *Powder Technology*, *281* (2015), Sept., pp. 129-137
[3] Wang, C, Zhu, J., Developments in the Understanding of Gas-Solids Contact Efficiency in the Circulating Fluidized Bed Riser Reactor: A review, *Chinese J. of Chemical Engineering, 24* (2015), 1, pp. 53-62
[4] Shabanian, J., Chaouki, J., Performance of a Catalytic Gas - Solid Fluidized Bed Reactor in the Presence of Interparticle Forces, *International Journal of Chemical Reactor Engineering*, *14* (2015), 1, pp. 433-444
[5] Shabanian, J., Chaouki, J., Influence of Interparticle Forces on Solids Motion in a Bubbling Gas-Solid Fluidized Bed, *Powder Technology*, *299* (2016), Oct., pp. 98-106
[6] Sun, G., Grace, J. R., Effect of Particle Size Distribution in Different Fluidization Regimes, *A. I. Ch. E. J*., *38* (1992), 5, pp. 716-722
[7] Edwards, M., Avidan, A., Conversion Model Aids Scale-Up of Mobil's Fluid-Bed MTG process, *Chemical Engineering Science*, *41* (1986), 4, pp. 829-835
[8] Foka, M., *et al*., Natural Gas Combustion in a Catalytic Turbulent Fluidized Bed, *Chem. Engng. Sci*., *49* (1994), 24, pp. 4269-4276
[9] Werther, J., 47 Modeling and Scale-Up of Industrial Fluidized Bed Reactors, *Chem. Engng. Sci*., *35* (1980), 1-2, 372-379
[10] Luo, H., *et al*., A Grid-Independent EMMS/Bubbling Drag Model for Bubbling and Turbulent Fluidization, *Chemical Engineering Journal*, *326* (2017), Oct., pp. 47-57
[11] Ayeni, O. O., *et al*., Development and Validation of a New Drag Law Using Mechanical Energy Balance Approach for DEM-CFD Simulation of Gas-Solid Fluidized Bed, *Chemical Engineering Journal*, *302* (2016), Oct., pp. 395-405
[12] Kia, S. A., Aminian, J., Hydrodynamic Modeling Strategy for Dense to Dilute Gas-Solid Fluidized Beds, *Particuology*, *31* (2017), Apr., pp. 105-116
[13] Venderbosch, R. H, *et al*., Platinum Catalyzed Oxidation of Carbon Monoxide as a Model Reaction in Mass Transfer Measurements, *Chem. Engng. Sci*., *53* (1998), 19, pp. 3355-3366
[14] Venderbosch, R. H., *et al.*, Mass Transfer and Influence of the Local Catalyst Activity on the Conversion in a Riser Reactor. *The Canadian Journal of Chemical Engineering*, *77* (1999), 2, pp. 262-274
[15] Venderbosch, R. H., The Role of Clusters in Gas-Solids Reactors. An Experimental Study, Enschede, Ph. D. Thesis Twente University, Enschede, The Netherlands, 1998
[16] Ranz ,W. E., Marshall, Jr. W. R., Evaporation from Drop: Part I, *Chem. Eng. Prog.*, *48* (1952), 3, pp. 141-146
[17] Ranz, W. E., Marshall, Jr. W. R., Evaporation from Drop: Part II, *Chem. Eng. Prog*., *48* (1952), 3, pp. 173-180
[18] Van der Ham, A. G. J., *et al*., Regenerative, High Temperature Desulfurization of Coal Gas in a Circulating Fluidized Bed, in Circulating Fluidized Bed Technology IV, Pennsylvania, Engineering Foundation, 657, 1994
[19] Kunii, D., Suzuki M., Particle-to-Fluid Heat and Mass Transfer in Packed Beds of Fine Particles, I*nt. J. Heat Mass Trans*., *10* (1967), 7, pp. 845-852
[20] Van Deemter, J. J., Mixing and Contacting in Gas-Solid Fluidized Beds, *Chem. Engng. Sci.*, *13* (1961), 3, pp. 143-154
[21] Sun, G., Grace, J. R., The Effect of Particle Size Distribution on the Performance of a Catalytic Fluidized Bed Reactor, *Chem. Engng. Sci.*, *45* (1990), 8, pp. 2187-2194

Paper submitted: July 7, 2018
Paper revised: April 10, 2019
Paper accepted: May 30, 2019